Polymers

Deutsche Ausgabe: DOI: 10.1002/ange.201412494
Internationale Ausgabe: DOI: 10.1002/anie.201412494

Molecularly Imprinted Polymer Nanomaterials and Nanocomposites: Atom-Transfer Radical Polymerization with Acidic Monomers**

*Zeynep Adali-Kaya, Bernadette Tse Sum Bui, Aude Falcimaigne-Cordin, and Karsten Haupt**

Abstract: *Molecularly imprinted polymers (MIPs) are artificial receptors which can be tailored to bind target molecules specifically. A new method, using photoinitiated atom-transfer radical polymerization (ATRP) for their synthesis as monoliths, thin films and nanoparticles is described. The synthesis takes place at room temperature and is compatible with acidic monomers, two major limitations for the use of ATRP with MIPs. The method has been validated with MIPs specific for the drugs testosterone and S-propranolol. This study considerably widens the range of functional monomers and thus molecular templates which can be used when MIPs are synthesized by ATRP, as well as the range of physical forms of these antibody mimics, in particular films and lithographic patterns, and their post-functionalization from living chain-ends.*

We describe herein a new method to synthesize molecularly imprinted polymer (MIP) nanomaterials and nanocomposites under mild reaction conditions. The reaction proceeds through photoinitiated atom-transfer radical polymerization (ATRP). MIPs, also referred to as "plastic antibodies", are synthetic biomimetic receptors which are capable of binding target molecules with an affinity and specificity similar to natural receptors such as enzymes and antibodies.[1] Molecular imprinting is based on the copolymerization of functional and crosslinking monomers in the presence of a molecular template. The removal of the template from the polymer matrix reveals specific recognition cavities which can then bind the target molecules (see Scheme S1 in the Supporting Information). MIPs are predominantly prepared by free-radical polymerization (FRP).[2] Controlled/living radical polymerization techniques, in contrast, can greatly improve the polymeric materials and are therefore a newly emerging and highly regarded approach in the molecular imprinting area. These sophisticated polymerization techniques not only allow the design of complex architectures and the modification of surface properties of MIPs, but also can result in an improved network morphology of the final polymers.[3,4] Hence, a more homogeneous distribution of molecular binding sites gives rise to enhanced molecular recognition properties.[5a,b]

ATRP is one of the most versatile controlled radical polymerization techniques and holds great promise for MIP synthesis. For instance, the group of Zhang demonstrated the surface modification of azobenzene-based photoresponsive MIPs with *N*-isopropylacrylamide, thus rendering the MIP particles thermoresponsive and hydrophilic.[6] These characteristics are important for the use of MIPs in aqueous environments, especially for applications in biotechnology and controlled drug release. Unfortunately, the use of ATRP in the MIP field has been limited thus far because of its inherent incompatibility with acidic monomers like methacrylic acid (MAA),[4] which is by far the most widely used functional monomer. Though there have been a few reports of MAA being employed in surface-initiated[7,8] or emulsion-type[9] ATRP for MIP synthesis, the technique was mainly used for the grafting of MIP films from surfaces, and the controlled/living character of the polymerization was not verified. Thus, ATRP with acidic monomers still constitutes a major limitation and a great challenge.

The metal catalyst has a prominent role in ATRP as it facilitates the redox reaction. It has therefore a great influence on maintaining control over the polymerization.[10–12] Considerable work has been devoted to catalyst development in the ATRP field,[13,14] with some recent efforts to develop photoinitiated ATRP.[15–17] Photoinitiated polymerization techniques pave the way to surface modification and patterning through lithography and enable synthesis of polymers at room temperature. Photopolymerization is also more versatile from a general point of view since it can be spatially controlled much more easily than thermal polymerization. For example, thin films and micropatterns can be obtained. It is also widely used for the synthesis of MIP micro- and nanostructures. Recently the group of Hawker employed *fac*-[Ir(ppy)$_3$] (ppy = 2-phenylpyridine) as an ATRP photoredox catalyst and maintained excellent control over the polymerization of methacrylates even in the presence of MAA.[18a] The *fac*-[Ir(ppy)$_3$] not only enabled the initiation of the reaction by visible light at room temperature, but because of its robustness it was also extremely tolerant to acidic moieties.

[*] Z. Adali-Kaya, Dr. B. Tse Sum Bui, Dr. A. Falcimaigne-Cordin, Prof. K. Haupt
Enzyme and Cell Engineering Laboratory
Compiègne University of Technology
CS60319, Rue Roger Couttolenc, 60205 Compiègne (France)
E-mail: karsten.haupt@utc.fr
Homepage: http://www.utc.fr/mip

[**] The authors thank the European Regional Development Fund ERDF for co-funding of the equipment under CPER 2007-2013, the European Commission (FP7 Marie Curie Actions, project CHEBANA, PITN-GA-2010-264772) for financial support and Frederic Nadaud from the physico-chemical analysis laboratory of Compiègne University for SEM and ESEM measurements. The Supporting Information is available online or from the authors. The authors declare no conflict of interest.

Supporting information for this article (experimental details: reagents and materials, synthesis, binding studies and characterization of MIPs) is available on the WWW under http://dx.doi.org/10.1002/anie.201412494.

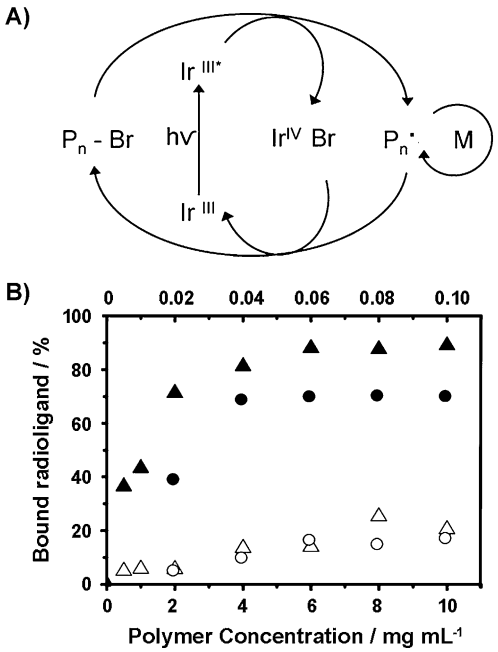

Figure 1. A) Proposed mechanism of ATRP with iridium photoredox catalyst (adapted from Ref. [18a], with permission). B) Equilibrium binding isotherms of [^{14}C]testosterone (80 pmol, 4.5 pCi) with bulk MIP (filled triangle) and NIP (empty triangle) in toluene (bottom axis), and of [^{3}H]propranolol (20 pmol, 15 nCi) with bulk MIP (filled circle) and NIP (empty circle) in acetonitrile (top axis). P_n = polymer chain, M = monomers.

The proposed polymerization mechanism with this catalyst is shown in Figure 1 A. Light is absorbed by *fac*-[Ir(ppy)$_3$], thus converting it into its excited state, *fac*-[Ir(ppy)$_3$]*.[18b,c] The latter then reduces an alkyl bromide initiator, thus resulting in the formation of the necessary alkyl radical for propagation, and in the oxidation of *fac*-[Ir(ppy)$_3$].[18a] This alkyl radical reacts with the highly oxidizing iridium(IV) complex forming the end-capped dormant polymer chain and iridium(III) complex in the ground state. This equilibrium process forms the basis of ATRP and enables the formation of living polymer chains with halide end-groups.

By using *fac*-[Ir(ppy)$_3$] as catalyst, we describe herein a new method to synthesize MIPs, at room temperature, through photoinitiated ATRP. This method is an important new development in the MIP field since it considerably widens the range of functional monomers and thus molecular templates which can be used when MIPs are synthesized by ATRP, as well as the range of physical forms of these MIPs. Also, avoiding higher temperatures is favorable for the stability of the template/monomer complex. MIPs composed of MAA as a functional monomer were produced in the form of monoliths, nanoparticles, and surface-bound films, thus demonstrating the versatility of the method. The drugs testosterone and S-propranolol were used as model templates. First, bulk polymers were synthesized using protocols adapted from previous publications.[19,20] MAA and ethylene glycol dimethacrylate (EGDMA) were used as monomers. MAA constituted 24 and 16 mol % of the total monomer amount in the testosterone and S-propranolol, respectively, MIP precursor solutions. Ethyl α-bromophenylacetate was the initiator, *fac*-[Ir(ppy)$_3$] was used as catalyst, and a 375 nm narrow-bandwidth light-emitting diode (LED) was employed as the light source. This wavelength corresponds to the maximum absorption of *fac*-[Ir(ppy)$_3$] (see Figure S1 in the Supporting Information). Polymerization was conducted at room temperature. Non-imprinted control polymers (NIPs) were prepared in the same manner except that the template was omitted. Polymer yields were determined to be 63 and 46 % for the testosterone MIP and NIP, respectively, and 89 and 75 % for propranolol MIP and NIP, respectively. The binding properties of the bulk polymers were evaluated by radioligand equilibrium binding assays. Both testosterone and S-propranolol imprinted polymers were very specific towards their corresponding analytes as evidenced by nearly no binding to the NIPs (Figure 1 B).

To evaluate the selectivity of the testosterone imprinted polymers, competitive binding assays at equilibrium were performed. The MIP was incubated with radiolabeled testosterone (80 nM) in the presence of structurally related compounds like β-estradiol, estrone, 1,4-androstene-3,17-dione, and 4-androstene-3,17-dione (see Figure S2 in the Supporting Information) at concentrations between 1 nM and 1 mM. The MIP exhibited negligible affinity for all of the related compounds, thus confirming its selectivity (see Figure S3 in the Supporting Information). The IC_{50} value (the concentration of competing ligand required to displace 50 % of the specifically bound radioligand) for testosterone, determined from a nonlinear regression fit was 3.8 μM, which is comparable to that obtained with MIPs synthesized through FRP.[19,21]

In the molecular imprinting field, commonly preferred ATRP catalysts are CuBr/*N*,*N*,*N*′,*N*″,*N*″-pentamethyldiethylenetriamine (PMDETA)[7,8,22–24] and CuBr/Tris[2-(dimethylamino)ethyl] amine (Me_6TREN).[6,25] It was thus interesting to compare their performance with that of *fac*-[Ir(ppy)$_3$]. MAA/EGDMA-based polymers were synthesized under reaction conditions (i.e., monomer concentrations and solvent) similar to those used for the testosterone polymers described above. The ATRP polymerizations employing CuBr/Me_6TREN and CuBr/PMDETA as catalysts were done at 60 °C for 48 hours. As expected, no polymerization was observed (see Figure S4 in the Supporting Information) because of the presence of the acidic monomer, thus indicating the superiority of *fac*-[Ir(ppy)$_3$] with acidic moieties.

To further demonstrate the efficiency of *fac*-[Ir(ppy)$_3$], it was employed to synthesize S-propranolol MIP nanoparticles (MIP-NPs) by precipitation polymerization. The same formulation used for the fabrication of bulk MIPs was adopted except that the volume of porogen was increased tenfold. The polymer yield was determined to be 46 and 20 % for MIP and NIP, respectively. The molecular recognition properties of the MIPs were found to be similar to their bulk counterparts (Figure 2 A). The particle size, as analyzed by scanning electron microscopy (SEM) was found to be about 45 nm (Figure 2 B). To assess the living character of the polymer chain-ends, acrylamide (AAm)-based polymer brushes were grafted from the halide-capped living ends of the MIP

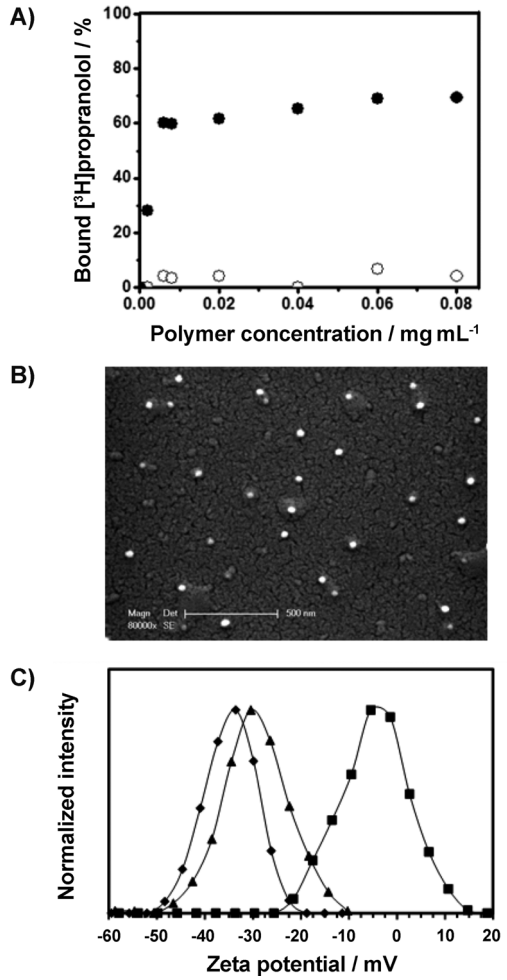

Figure 2. A) Equilibrium binding isotherms of [^{3}H]propranolol (20 pmol, 15 nCi) with MIP (filled circle) and NIP (empty circle) nanoparticles in acetonitrile. B) Scanning electron micrograph of S-propranolol imprinted MIP particles obtained by ATRP of MAA and EGDMA in acetonitrile C) Zeta potential measurements of S-propranolol MIP particles based on MAA/EGDMA cores (diamonds), AAm-modified MIP particles (squares), and core-AAm-EGMP particles (triangles) in 20 mM sodium phosphate buffer pH 8.0.

nanoparticles (Scheme 1 A). The MIP nanoparticles were dispersed in acetonitrile (ACN) and irradiated with the 375 nm LED in the presence of *fac*-[Ir(ppy)$_3$] and AAm, without the addition of any initiator, for 2 hours at room temperature. The formation of the poly-AAm brushes was indicated by the change in zeta potential from −33 mV (core MIP-NPs) to −5 mV (Figure 2 C). We were also able to further functionalize the particles with negatively charged ethylene glycol methacrylate phosphate (EGMP) by using the iridium-based catalyst (Scheme 1 A). Phosphorus-containing charged polymers are of interest in the biomaterials field, especially in tissue engineering[26] where they provide biocompatibility, allow integration with the bone, improve cell attachment, and enhance the mineralization processes.

Core-AAm-EGMP particles were fabricated by exposing the core-AAm particles to the 375 nm LED light source in the presence of *fac*-[Ir(ppy)$_3$] and EGMP for 2 hours in ACN. Polymers grafted with EGMP exhibited a negative zeta potential shift from −5 mV to −30 mV (Figure 2 C), thus confirming the living character of the MIPs. Further proof of EGMP grafting was obtained by energy-dispersive X-ray spectroscopy (EDS) analysis. The element phosphorous, present in EGMP, was clearly observed as the P peak (see Figure S5c in the Supporting Information). The spectrum of the core particles does not contain a P peak, and the spectrum of the core-AAm particles contains a negligible P peak.

To further demonstrate the versatility of the photocatalyst *fac*-[Ir(ppy)$_3$], ATRP was applied for surface grafting (Scheme 1 B). For this study, an MAA/EGDMA-based cross-linked copolymer layer was grown from a gold surface after attaching the initiator by diazonium salt chemistry, which results in a stable metal–carbon bond. This bond is an advantage over the more common thiol link which is not stable under UV irradiation.[27] A diazonium salt bearing an alcohol functionality was first synthesized according to a protocol from the literature[25] (see the Supporting Information). Bromo-active moieties were then introduced through treatment with 2-bromopropionyl bromide (see Scheme S2 in the Supporting Information). MAA/EGDMA-based copolymers were synthesized by irradiation

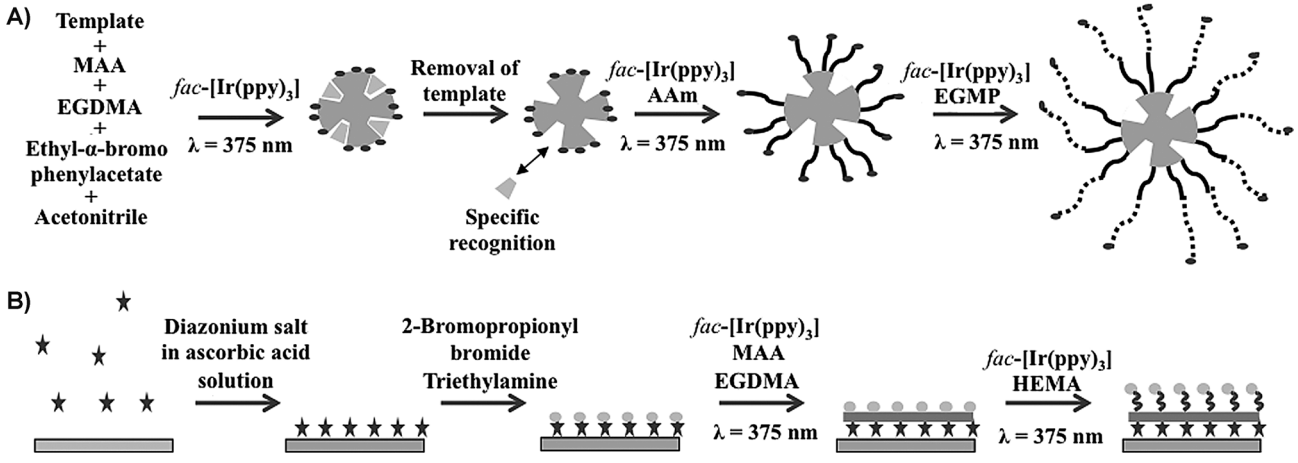

Scheme 1. A) Synthesis of MIP particles with chain-end functionality and further modification by grafting polymer brushes from particles. B) Fabrication of surface-bound polymer films and their modification by grafting polymers.

at 375 nm in presence of *fac*-[Ir(ppy)$_3$]. The thickness of the polymer was determined to be 12 nm by atomic force microscopy (AFM; see Figure S6a in the Supporting Information). The surface of the polymers was further modified by irradiation at 375 nm in the presence of a hydrophilic monomer 2-hydroxyethyl methacrylate (HEMA) and *fac*-[Ir(ppy)$_3$]. The thickness of the polymer was increased to 52 nm (see Figure S6b). The success of the grafting was confirmed by a change in wettability of the surface, as studied by microcondensation of water observed by environmental scanning electron microscopy (ESEM). Water microdroplets on an MAA/EGDMA thin polymer layer had a shape characteristic for a high contact angle and thus a hydrophobic surface and bad wetting (see Figure S7a in the Supporting Information). Upon coating the MAA/EGDMA layer with HEMA from the living chain-ends of the MAA/EGDMA, the surface became hydrophilic as evidenced by visual observation of larger water drops with decreased thickness (see Figure S7b), which is characteristic for good wetting.

In conclusion, we demonstrated a new method to synthesize MIPs in the form of monoliths, nanoparticles, and surface-bound films, through photoinitiated ATRP using *fac*-[Ir(ppy)$_3$] as the catalyst. MIPs based on MAA as a functional monomer were synthesized for specific binding of testosterone and S-propranolol. The living character of the polymerization was demonstrated by postmodifications from functionalized chain-ends. Polymer brushes were grafted from MIP nanoparticles and surface-bound polymer films, thus enabling the tuning of their surface charge. This development is very important since it considerably widens the range of functional monomers and thus molecular templates which can be used when MIPs, as antibody mimics, are synthesized by ATRP. Additionally, the range of physical forms of these MIPs and their applications also increase.

Keywords: diazo compounds · molecular imprinting · iridium · living polymerization · ATRP

How to cite: *Angew. Chem. Int. Ed.* **2015**, *54*, 5192–5195
Angew. Chem. **2015**, *127*, 5281–5284

[1] K. Haupt, A. Linares, M. Bompart, B. Tse Sum Bui in *Topics in Current Chemistry*, *Vol. 325* (Ed.: K. Haupt), Springer, Berlin, **2012**, chap. 1.
[2] L. Chen, S. Xu, J. Li, *Chem. Soc. Rev.* **2011**, *40*, 2922.
[3] V. D. Salian, M. E. Byrne, *Macromol. Mater. Eng.* **2013**, *298*, 379.
[4] M. Bompart, K. Haupt, *Aust. J. Chem.* **2009**, *62*, 751.
[5] a) H. Zhang, *Eur. Polym. J.* **2013**, *49*, 579; b) C. Gonzato, P. Pasetto, F. Bedoui, P.-E. Mazeran, K. Haupt, *Polym. Chem.* **2014**, *5*, 1313.
[6] L. Fang, S. Chen, X. Guo, Y. Zhang, H. Zhang, *Langmuir* **2012**, *28*, 9767.
[7] J. Liu, W. Wang, Y. Xie, Y. Huang, Y. Liu, X. Liu, R. Zhao, G. Liu, Y. Chen, *J. Mater. Chem.* **2011**, *21*, 9232.
[8] X. Li, J. Pan, J. Dai, X. Dai, H. Ou, L. Xu, C. Li, R. Zhang, *J. Sep. Sci.* **2012**, *35*, 2787.
[9] J. Dai, J. Pan, L. Xu, X. Li, Z. Zhou, R. Zhang, Y. Yan, *J. Hazard. Mater.* **2012**, *205–206*, 179.
[10] K. Matyjaszewski, J. Xia, *Chem. Rev.* **2001**, *101*, 2921.
[11] M. Kamigaito, T. Ando, M. Sawamoto, *Chem. Rec.* **2004**, *4*, 159.
[12] N. V. Tsarevsky, K. Matyjaszewski, *Chem. Rev.* **2007**, *107*, 2270.
[13] M. Ouchi, T. Terashima, M. Sawamoto, *Chem. Rev.* **2009**, *109*, 4963.
[14] T. Pintauer, K. Matyjaszewski, *Coord. Chem. Rev.* **2005**, *249*, 1155.
[15] D. Konkolewicz, K. Schröder, J. Buback, S. Bernhard, K. Matyjaszewski, *ACS Macro Lett.* **2012**, *1*, 1219.
[16] M. A. Tasdelen, M. Uygun, Y. Yagci, *Macromol. Chem. Phys.* **2011**, *212*, 2036.
[17] M. Ciftci, M. A. Tasdelen, W. Li, K. Matyjaszewski, Y. Yagci, *Macromolecules* **2013**, *46*, 9537.
[18] a) B. P. Fors, C. J. Hawker, *Angew. Chem. Int. Ed.* **2012**, *51*, 8901; *Angew. Chem.* **2012**, *124*, 9031; b) H.-W. Shih, M. N. Vander Wal, R. L. Grange, D. W. C. MacMillan, *J. Am. Chem. Soc.* **2010**, *132*, 13600; c) A. McNally, C. K. Prier, D. W. C. MacMillan, *Science* **2011**, *334*, 1114.
[19] B. Tse Sum Bui, F. Merlier, K. Haupt, *Anal. Chem.* **2010**, *82*, 4420.
[20] C. Gonzato, M. Courty, P. Pasetto, K. Haupt, *Adv. Funct. Mater.* **2011**, *21*, 3947.
[21] B. Tse Sum Bui, K. Haupt, *J. Mol. Recognit.* **2011**, *24*, 1123.
[22] B. Zu, G. Pan, X. Guo, Y. Zhang, H. Zhang, *J. Polym. Sci. Part A* **2009**, *47*, 3257.
[23] B. Zu, Y. Zhang, X. Guo, H. Zhang, *J. Polym. Sci. Part A* **2010**, *48*, 532.
[24] H. Zhang, J. Jiang, H. Zhang, Y. Zhang, P. Sun, *ACS Macro Lett.* **2013**, *2*, 566.
[25] S. Gam-Derouich, M. N. Nguyen, A. Madani, N. Maouche, P. Lang, C. Perruchot, M. M. Chehimi, *Surf. Interface Anal.* **2010**, *42*, 1050.
[26] C. R. Nuttelman, D. S. W. Benoit, M. C. Tripodi, K. S. Anseth, *Biomaterials* **2006**, *27*, 1377.
[27] M. Gu, J. E. Kilduff, G. Belfort, *Biomaterials* **2012**, *33*, 1261.

Received: December 31, 2014
Revised: February 11, 2015
Published online: February 27, 2015

